

On Pressure Gradients and Rapid Migration of Solids in an Inhomogeneous Solar Nebula

Nader Haghighipour and Alan P. Boss

*Department of Terrestrial Magnetism, Carnegie Institution of Washington,
5421 Broad Branch Road, Washington, DC 20015*

nader@dtm.ciw.edu, boss@dtm.ciw.edu

ABSTRACT

We study the motions of small solids, ranging from micron-sized dust grains to 100-m objects, in the vicinity of a local density enhancement of an isothermal gaseous solar nebula. Being interested in possible application of the results to the formation of clumps and spiral arms in a circumstellar disk, we numerically integrate the equations of motion of such solids and study their migration for different values of their sizes and masses and also for different physical properties of the gas, such as its density and temperature. We show that, considering the drag force of the gas and also the gravitational attraction of the nebula, it is possible for solids, within a certain range of size and mass, to migrate rapidly (i.e. within ~ 1000 years) toward the location of a local maximum density where collisions and coagulation may result in an accelerated rate of planetesimal formation.

Subject headings: solar system: formation, planetary systems: formation, planetary systems: protoplanetary disks

1. Introduction

It is generally believed that planet formation starts as a secondary process to star formation by coalescence of small bodies in circumstellar disks. With regard to our solar system, two mechanisms have been proposed for the formation of the giant planets in such a disk around our Sun; the widely accepted core accretion model (Pollack et al. 1996) and the disk instability scenario (Boss 2000). It has recently been noted that a solar nebula massive enough to possibly form giant planets via the core accretion model is likely marginally-gravitationally unstable (Pollack et al. 1996; Boss 2000; Inaba and Wetherill

2002). The alternative approach, namely the disk instability mechanism, however, implies that such an instability could lead to rapid formation of gas giant planets. It is, therefore, of great importance to study how the dynamics of small solids will be affected in such an unstable environment, and what implications there will be on the collision and coagulation process.

In general, in a non-turbulent, freely rotating gaseous disk at hydrostatic equilibrium, there is a radial gradient associated with the gas pressure. This pressure gradient counteracts the gravitational attraction of the central star and causes the gas molecules to have slightly different velocities than Keplerian circular. When the pressure gradient is positive, the velocity of a gas molecule is greater than the local Keplerian velocity. A solid in the gas, in this case, feels an acceleration by the gas along its orbit and, consequently, the increase in its orbital angular momentum forces the solid to a larger orbit. In this case, we say that the solid feels a “tail wind.” The opposite is true when the pressure gradient is negative. That is, a solid body will be subject to a “head wind” and will migrate toward smaller orbits.

One of the features of a rotating gravitationally unstable disk is the appearance of spiral arms or clumps where the density of the medium is locally enhanced. In the vicinity of such density enhancements, the pressure of the gas may change radially and cause the particles in the disk to migrate toward the location of the maximum gas density. We are interested in studying the dynamics of solids that undergo such migration and in exploring the possibility of applying the results to the formation of planetesimals in a marginally-gravitationally unstable disk. As the first stage of our project, we present here the results of a systematic study of the migration of solids subject to gas drag and the gravitational force of a circumstellar disk, around the location of its maximum density. To focus attention on the dynamics of the solids and its association with parameters such as the temperature of the gas, the sizes of the objects, and also the values of their densities, we consider a hypothetical solar nebula with a circularly symmetric density function.

Studies of the motions of solids in gaseous mediums have been presented by many authors. In a detailed analytical analysis in 1962, Kiang studied the dynamical evolution of solids in elliptical orbits subject to resistive forces proportional to arbitrary powers of their relative velocities and their distances to the star. In his study, Kiang considered three cases of stationary, uniformly rotating, and also freely rotating gaseous mediums. However, he did not consider the pressure gradient of the gas. It was Whipple (1964) who first mentioned that the rotation of the solar nebula deviates from Keplerian because of counterbalancing the gravity of the Sun by the internal pressure of the gas which in turn results in in/outward migration of small solids. In 1972, Whipple studied the dynamics of such solids in the solar nebula where, following an approximation by Probst and Fässio (1969), he also

included the resistive effect of the gas. Whipple’s work was subsequently expanded upon and generalized by Weidenschilling (1977) for a variety of model nebulae and different sizes of solids.

A comprehensive study of the effect of gas drag on the motions of solid bodies can also be found in the classic work of Adachi et al. (1976). In their paper, Adachi et al. studied the motion of a solid on an elliptical orbit in a solar nebula whose density and temperature vary inversely with different powers of the distance from the Sun. They also presented a detailed analysis of the form of the gas drag for different relative velocities and relative sizes of solids, and also different values of the gas Reynolds number.

Among the more recent studies of the dynamical evolution of solids in a gaseous disk, one can name the work of Malhotra (1993) on resonance capture of planetesimals subject to a drag force proportional to their relative velocities, as a barrier for the inward flow of solids to the accretion zone of a planetary embryo in the solar nebula, a paper by Supulver and Lin (2000) on the formation of icy planetesimals subject to a linear combination of Stokes and Epstein drags in an azimuthally symmetric, turbulent and thin solar nebula with a polytropic equation of state, and also a paper by Iwasaki, Tanaka and Emori (2001) on the stability/instability of protoplanets subject to gas drag.

In this paper, we study the dynamics of solid bodies in an inhomogeneous gaseous disk. Our model nebula consists of a Sun-like star at its center and non-interacting collisionless bodies scattered on its midplane. We consider the effect of drag force and also include the gravitational attraction of the nebula.

The outline of this paper is as follows. Section 2 introduces the equations of motion and also the basic relations concerning drag and the gravitational force of the gas. Section 3 defines the system of interest, and section 4 presents the results of our numerical simulations. Section 5 concludes this study by reviewing the results and discussing their applications.

2. Basic Relations

We consider a thin, isothermal and freely rotating gaseous disk with a Sun-like star at the center of its midplane. A solid object in this medium, in addition to the gravitational force of the central star, is subject to gas drag and also to the gravitational attraction of the disk. In a inertial coordinate system with its origin at the position of the star and its axes on the midplane of the nebula, the equation of motion of such a solid can be written as

$$m_p \ddot{\mathbf{r}}_p = -GMm_p \left(\frac{\mathbf{r}_p}{r_p^3} \right) + \mathbf{F}_{\text{drag}} + \mathbf{F}_{\text{disk}} , \quad (1)$$

where m_p and \mathbf{r}_p represent the mass and the position vector of the solid, M is the mass of the central star and G is the gravitational constant. The quantities \mathbf{F}_{drag} and \mathbf{F}_{disk} in equation (1) denote the gas drag and the gravitational force of the nebula, respectively. In the following, we discuss these two forces in detail.

2.1. Gas Drag

In general, the drag force of a gaseous medium with a density ρ_g on a spherical body with radius a_p is proportional to the square of its relative velocity, \mathbf{V}_{rel} , and is given by (Landau and Lifshitz 1959; Adachi et al. 1976)

$$\mathbf{F}_{\text{drag}} = -\frac{1}{2}C_D\pi a_p^2\rho_g v_{\text{rel}}\mathbf{V}_{\text{rel}}. \quad (2)$$

In this equation, $v_{\text{rel}} = |\mathbf{V}_{\text{rel}}|$ and C_D , the drag coefficient, is a dimensionless constant that depends on the gas Reynolds number, the ratio of the relative velocity of the solid to the speed of sound in the medium (the Mach number), and also the relative size of the solid compared to the mean free path of the gas molecules (the Knudsen number). For a detail analysis of the drag coefficient we refer the reader to Adachi et al. (1976).

For the cases where the mean free path of the gas molecules is smaller than the size of the object, we have (Whipple 1972; Weidenschilling 1977)

$$C_D \simeq \begin{cases} 24 Re^{-1} & \text{if } Re < 1 \text{ (Stokes' drag)} \\ 24 Re^{-0.6} & \text{if } 1 < Re < 800 \\ 0.44 & \text{if } Re > 800, \end{cases} \quad (3)$$

where Re is the gas Reynolds number. For a gas with a viscosity ν ,

$$Re = \frac{2}{\nu} \rho_g a_p v_{\text{rel}}, \quad (4)$$

and

$$\nu = \frac{1}{3} \left(\frac{m_0 \bar{v}_{\text{th}}}{\sigma} \right), \quad (5)$$

where m_0 and \bar{v}_{th} represent the mass and the mean thermal velocity of the gas molecules and σ is their collisional cross section (Adachi et al. 1976; Weidenschilling 1977).

For particles moving much slower than the gas mean thermal velocity and with sizes smaller than the mean free path of the gas molecules, \mathbf{F}_{drag} can be approximately written as

$$\mathbf{F}_{\text{drag}} = -\frac{4}{3}\pi\rho_g a_p^2 v_{\text{th}} \mathbf{V}_{\text{rel}}. \quad (6)$$

Equation (6) is known as Epstein drag (Kennard 1938; Epstein 1924).

As shown by equations (2) and (6), the resistive effect of the gas is directly proportional to the size of solids. Anticipating numerically integrating equation (1) for different values of a_p , we follow Supulver and Lin (2000) and combine equations (2) and (6) by introducing $f = a_p/(a_p + \ell)$ where ℓ is the mean free path of the gas molecules. We now write

$$\mathbf{F}_{\text{drag}} = -\frac{4}{3}\pi a_p^2 \rho_g \left[(1-f)\bar{v}_{\text{th}} + \frac{3}{8}f C_D v_{\text{rel}} \right] \mathbf{V}_{\text{rel}}, \quad (7)$$

which is particularly useful for transitional cases where the size of solids and the mean free path of the gas molecules are comparable. In equation (7), $\mathbf{V}_{\text{rel}} = \mathbf{V}_p - \mathbf{V}_g$ where \mathbf{V}_p is the velocity of a solid and \mathbf{V}_g , the velocity of the gas at the location of the solid, has a magnitude given by

$$v_g^2 = \frac{GM}{r_p} + \frac{r_p}{\rho_g(\mathbf{r}_p)} \left(\frac{dP_g}{dr} \right)_{\mathbf{r}=\mathbf{r}_p}. \quad (8)$$

In this equation, P_g is the pressure of the gas. As shown in equation (8), the velocity of the gas slightly differs from its Keplerian circular value (first term of the right hand side) due to the pressure gradient.

2.2. Gravitational Potential of the Disk

As mentioned earlier in this section, the model nebula considered here is a gaseous disk with a radius much larger than its thickness. Although thin, this nebula has a considerable thickness compared to the size of the solids of our interest. Therefore, in addition to the drag forces and the gravitational attraction of the central star, objects in this nebula feel a force associated with the gravitational potential of the disk. In this section, we present a brief analytical analysis of the calculation of the gravitational force of the above-mentioned nebula. Detailed analysis is in preparation for publication elsewhere.

As seen by a solid in the nebula, the gaseous disk surrounding the central star resembles a thin cylinder with a considerably large radius. The gravitational force of the nebula on a

solid is equal to the gradient of the gravitational potential of this cylinder at the location of the solid. This potential function, denoted by $\phi(\mathbf{R})$, satisfies Poisson's equation. That is,

$$\nabla^2 \phi(\mathbf{R}) = 4\pi G \rho_g(\mathbf{R}). \quad (9)$$

In this equation, \mathbf{R} is the solid's three dimensional position vector in a general coordinate system with an origin at the position of the central star. For the system of interest in this paper, it is possible to reduce the partial differential equation (9) into a more manageable form. As mentioned in section 1, we consider ρ_g to be circularly (azimuthally) symmetric. We also assume that the motions of solids are restricted to the midplane of the nebula. Since the thickness of the disk is much larger than the size of the solids, the latter assumption implies that the change of the gravitational potential of the gas along the diameter of a solid perpendicular to the midplane of the nebula can be considered negligible. Combined with the azimuthal symmetry of ρ_g , in a cylindrical coordinate system with its origin on the central star and its plane-polar components measured on the midplane of the nebula, the simplifying assumption above allows us to write equation (9) as

$$\frac{1}{r} \frac{d}{dr} \left(r \frac{d\phi}{dr} \right) = 4\pi G \rho_g(r), \quad (10)$$

where r is the plane-polar component of \mathbf{R} . The gravitational force associated with potential $\phi(\mathbf{R})$ is equal to $-m\nabla\phi(\mathbf{R})$ and for a particle restricted to move on the midplane of the nebula is given by

$$\mathbf{F}_{\text{disk}}(\mathbf{r}) = -\frac{4\pi}{r^2} G m \left[\int \rho_g(r') r' dr' - c \right] \mathbf{r}, \quad (11)$$

where c is the constant of integration whose value is calculated from the dynamical properties of the system.

2.3. Equation of Motion

The equation of motion of a solid in this study is given by equation (1). For the purpose of numerical integrations, it is more convenient to write this equation in a dimensionless form. Introducing the quantities r_0 and t_0 which carry the dimensions of length and time, respectively, equation (1) can be written as

$$\ddot{\hat{\mathbf{r}}} = -\hat{k}\left(\frac{\hat{\mathbf{r}}}{\hat{r}^3}\right) + \hat{\mathbf{F}}_{\text{drag}} + \hat{\mathbf{F}}_{\text{disk}}. \quad (12)$$

where $\mathbf{r}_p = r_0 \hat{\mathbf{r}}$, $t = t_0 \hat{t}$, $\hat{k} = GMt_0^2/r_0^3$ and a general dimensionless force $\hat{\mathbf{F}}$ is equal to $t_0^2 \mathbf{F}/m_p r_0$. We choose r_0 and t_0 such that $\hat{k} = 1$. For a solid restricted to move on the midplane of the nebula, equation (12), in a dimensionless form and in a plane-polar coordinate system with axes on the midplane of the disk, is written as

$$P_r = \dot{r}, \quad (13)$$

$$P_\theta = r^2 \dot{\theta}, \quad (14)$$

$$\dot{P}_r = \frac{1}{r^3} P_\theta^2 - \frac{1}{r^2} - \frac{1}{r} \left[4\pi \int \tilde{\rho}_g(r') r' dr' - c \right] - \frac{4}{3} \pi a_p^2 \hat{\rho}_g(r) P_r \left[(1-f) \bar{v}_{\text{th}} + \frac{3}{8} f C_D v_{\text{rel}} \right], \quad (15)$$

$$\dot{P}_\theta = -\frac{4}{3} \pi r a_p^2 \hat{\rho}_g(r) (v_{\text{rel}}^2 - P_r^2)^{1/2} \left[(1-f) \bar{v}_{\text{th}} + \frac{3}{8} f C_D v_{\text{rel}} \right], \quad (16)$$

where P_r and P_θ are, respectively, the radial and the angular momenta of the solid, $\hat{\rho}_g = r_0^3 \rho_g(r)/m_p$, and $\tilde{\rho}_g = r_0^3 \rho_g(r)/M$. In equations (13) to (16), the hat signs have been dropped for simplicity.

3. The Physical Model

We consider a gaseous nebula of pure molecular hydrogen with a uniform temperature T and a density given by

$$\rho_g(r) = \rho_0 e^{-\alpha(r-r_m)^2}. \quad (17)$$

In equation (17), ρ_0 is the magnitude of the local maximum of the density and r_m denotes its radial position. The coefficient α in this equation is a positive constant. Figure 1 shows $\rho_g(r)$ for $\alpha = 0.5$ and 1. It is necessary to emphasize that the choice of density, as given by equation (17), has been made, solely, to focus attention on the effects of the pressure gradient, gas drag and also the gravitational force of the disk on migration of solids and their dynamics. In a more realistic system, the density of the gas will have a much more complicated form. Extension of this work to such cases is the subject of up-coming articles.

As mentioned earlier, we would like to study the dynamics of a solid in a gaseous disk with a density given by equation (17) by numerically simulating its motion given by equations (13) to (16). These equations require us to write certain quantities such as the pressure of the gas, its mean thermal velocity, the mean free path of its molecules and also the relative velocity of the solid, in terms of the gas density ρ_g . To do so, we assume that our model

nebula obeys the equation of state of an ideal gas, $P_g = nk_B T$, where n is the gas number density and k_B is the Boltzmann's constant. The mean thermal velocity of the gas molecules is, therefore, given by

$$\bar{v}_{\text{th}}^2 = \frac{8k_B T}{\pi m_0}. \quad (18)$$

Substituting for T from the ideal gas law in equation (18), the pressure of the gas will be equal to

$$P_g = \frac{1}{8} \pi \bar{v}_{\text{th}}^2 \rho_g(r). \quad (19)$$

From this equation and in a dimensionless form, the relative velocity of a solid can be written as

$$v_{\text{rel}}^2 = P_r^2 + \left[\frac{P_\theta}{r} - \left(\frac{1}{r} + \frac{\pi r \bar{v}_{\text{th}}^2}{8 \rho_g(r)} \frac{d\rho_g(r)}{dr} \right)^{1/2} \right]^2. \quad (20)$$

The mean free path of the gas molecules can also be written in terms of ρ_g . Assuming a diameter of a_0 for the gas molecules, $\ell = 1/(\pi a_0^2 n)$. From the ideal gas law and also from equation (18), one can write

$$\ell = \frac{m_0}{\pi a_0^2 \rho_g(r)}. \quad (21)$$

For molecular hydrogen, $a_0 = 1.5 \times 10^{-8}$ cm. The mean free path of the molecules of our model nebula can, therefore, be written as, ℓ (cm) = $4.72 \times 10^{-9} / \rho_g(r)$ (g cm^{-3}).

The gravitational attraction of the disk as given by equation (11) requires us to calculate the integral $\int \rho_g(r) r dr$ and also the constant of integration c . Using equation (17), the integral of equation (11) will be equal to

$$\int \tilde{\rho}_g(r') r' dr' = \frac{1}{2} \alpha^{-1/2} \tilde{\rho}_0 \left\{ r_m \pi^{1/2} \text{Erf}[\alpha^{1/2}(r - r_m)] - \alpha^{-1/2} e^{-\alpha(r - r_m)^2} \right\}, \quad (22)$$

where $\tilde{\rho}_0 = r_0^3 \rho_0 / M$ and $\text{Erf}(r)$ is the error function. As mentioned in section 2.2, the constant of integration c depends on the dynamical properties of the system. In our physical model with a density function given by equation (17), the radial migration of solids due to the pressure gradient terminates at $r = r_m$. That is, a solid object at position r_m will stay with the gas and, consequently, its relative velocity will become zero. That implies, at the location of the maximum density of the gas, $\mathbf{F}_{\text{drag}} = 0$. Also, because we assumed that the

disk is rotating freely, a solid at $r = r_m$ will rotate the central star in a circular orbit. That means, at this position, $\dot{r} = 0$. Applying these two conditions to equation (22), we have

$$c = \frac{1}{r_m} - r_m^2 \dot{\theta}_{(r=r_m)}^2 - \frac{2\pi\tilde{\rho}_0}{\alpha}, \quad (23)$$

where all quantities have been written in a dimensionless form.

4. Numerical Simulations

We consider a gas density given by equation (17) with a peak equal to $10^{-9} \text{ g cm}^{-3}$ at $r_m = 1 \text{ AU}$. The value of α is considered as a parameter in our simulations. As mentioned in section 3, we choose our units such that $\hat{k} = 1$. Therefore, the quantities r_0 and t_0 are related as $t_0^2 = r_0^3/GM$. Introducing a new variable $T_0 = 2\pi t_0$, we have

$$T_0 = 2\pi \left(\frac{r_0^3}{GM} \right)^{1/2}. \quad (24)$$

Equation (24) implies that T_0 can be considered as the period of an object rotating uniformly around the star M on a circular path with radius r_0 . In our physical model, an object at $r = r_m$ has such a uniform circular motion. We set $r_0 = r_m = 1 \text{ AU}$ and, therefore, from equation (24), $t_0 \simeq 5.03 \times 10^6 \text{ sec} \simeq 0.16 \text{ years}$. Also in this case, $\dot{\theta}(r_m = 1 \text{ AU}) = 1$ and $c \simeq -0.0106 \alpha^{-1}$.

We numerically integrated equations (13) to (16) for different values of the gas temperature, solids' radii and densities, and also different values of α . Figure 2 shows the radial migration of solids ranging from micron-sized particles to 100 m objects from 2 AU and 0.25 AU to the location of the peak of the density of Figure 1 with $\alpha = 1$. The densities of the objects are equal to 2 g cm^{-3} . As expected, small particles spend more time with the gas and take a longer time to migrate in/outward. As the sizes of the particles increase, while their densities stay constant, the rate of radial migration also increases. Figure 3 shows a comparison of the times of migration for four different values of the initial orbital radii of the solids of Figure 2. One can see from this figure that for the above-mentioned physical properties of the gas and solids, the graphs of the 10 cm and 1 m objects show the most rapid radial migration, comparable to the timescale of the growth of non-axisymmetries in disk instability models. Increasing the radius of the solid to 10 m or higher, one observes that the rate of migration decreases again.

Figure 3 also shows that the rates of inward and outward migrations for equal distances at both sides of $r = 1$ AU are different. The inward migrations from 1.75, 1.5 and 1.25 AU occur more rapidly than the outward migrations from 0.25, 0.5 and 0.75 AU. To explain these differences, we have plotted the relative velocity of a particle (Eq. [20]) during its migration. Figure 4 shows the magnitude of \mathbf{V}_{rel} for a 1 m-sized object with a density equal to 2 g cm^{-3} migrating from $r = 1.75$ or 0.25 AU to $r = 1$ AU. The temperature of the gas is 1000 K. As shown here, the magnitude of the relative velocity of the object when approaching $r = 1$ AU from a larger distance is greater than its relative velocity when migrating out. One can explain this, qualitatively, by studying equation (20) in more details. From Figure 1, the quantity $d\rho_g(r)/dr$, the contribution of the pressure gradient, is negative for distances larger than 1 AU and positive for smaller distances. When migrating in/outward, the absolute value of the quantity above decreases while its sign stays the same. Since the contribution of the pressure gradient in case of an outward migration is positive, the second term inside the square brackets of equation (20) will have larger values for outward migrations resulting in smaller values for the second term of equation (20) and, consequently, smaller relative velocities in these cases. From equation (2), this implies that resistive effect of the headwind felt by the solid during its inward migrating is larger than the effect of the tailwind that causes its outward motion. In other words, the inward migration of the solid is accomplished faster.

The rate of radial migration varies also with the density of solids. Figure 5 shows the migrations of solids with radii from 1 cm to 10 m for three different values of the solid's density. The physical properties of the gas in this figure are identical to Figure 1. As shown in Figure 5, for $a_p = 1$ and 10 cm, the rate of radial migration increases by increasing the solid's density. The reason for this can be found in the contribution of the drag force (Eq. [7]) to the change of the radial momentum of the solid given by equation (15). We recall that in the latter equation, $\hat{\rho}_g$ is a dimensionless quantity whose numerical value is equal to $\rho_g r_0^3 / m_p$. For a constant value of a_p , increasing the density of the object will result in increasing its mass and, consequently, decreasing the dimensionless density $\hat{\rho}_g$. As a result, the last term of equation (15) will have a smaller absolute value and, therefore, the radial momentum of the object will have a larger rate. That is, its radial migration will be faster.

The above-mentioned feature does not sustain for larger values of the solids radii. When $a_p \geq 1$ m, both the inward and the outward migrations slow down when the densities of solids are increased. This can also be attributed to the behavior of the last term of equation (15) for these values of a_p . Recall that from equation (21), for the range of r considered here (i.e., $0.25 \leq r \leq 2$), the maximum value of the mean free path of the gas molecules is approximately 12.8 cm. That means, for the values of the solids radii larger than 1 m, the coefficient f is approximately equal to one. The contribution of the drag force of the gas to

the time variation of the radial momentum of the solids given by the last term of equation (15), in this case, will be proportional to a_p , $a_p^{1.4} \rho_g^{0.4}$, and $a_p^2 \rho_g$ for different values of the drag coefficient C_D given by equation (3). It is evident that for meter-sized and larger objects, the last term of equation (15) will have larger absolute values resulting in smaller values for \dot{P}_r and, consequently, slower radial migration.

Numerical integrations have also been carried out for different values of the temperature of the gas. The effect of a change in temperature appears in the thermal velocity of the gas which in turn results in changes in the value of the gas viscosity and eventually its drag coefficient, and also affects the pressure gradient and the relative velocity of the solids. Figure 6 shows the rate of migration of a 10 cm-sized solid with a density of 2 g cm^{-3} for two values of $\alpha = 0.5$ and 1. As shown here, by increasing the temperature, the time of migration toward the location of the maximum density increases. This can be attributed to the fact that an increase in the temperature of the gas will increase the mean thermal velocity of its molecules and, therefore, from equation (20), will result in smaller values of the relative velocity of the solid. The drag force of the gas, in this case, will have a smaller magnitude (see eq. [2]) implying that when migrating inward at a higher temperature, the drag force will need more time to slow down the object and when migrating outward, the import of angular momentum to the particle via a tailwind generated by the gas drag will be smaller. Figure 7 shows a comparison between the magnitude of the relative velocity of a 10 cm particle migrating inward from 2 AU and outward from 0.25 AU at 1000 K and 300 K. One can see from this figure that for both cases of inward and outward migrations, the magnitude of the relative velocity is larger for a smaller temperature.

Although the above-mentioned features are observed in the motion of a solid in both cases of $\alpha = 0.5$ and 1, a comparison between the graphs of these two values of α indicates that for each value of the temperature, the time of migration is longer for smaller values of α , a result that is evident from the density distribution shown in Figure 1; smaller values of α corresponds to smaller gas pressure gradients.

5. Summary and Discussion

We have studied motions of small solids in the vicinity of a density enhancement in a freely rotating gaseous disk. We assume that the gas is isothermal and ideal. In this case, an enhancement in the gas density corresponds to a maximum in its pressure. As expected, because of the pressure gradient associated with the radial change of the gas density, solids on both sides of the location of the maximum pressure (or density) undergo

in/outward migrations. We have studied such migrations in a model solar nebula where solids, in addition to the gravitational attraction of the central star, are subject to gas drag and to the gravitational force of the nebular disk.

In general, the rate of the migration of a solid in a gaseous medium due to the pressure gradient varies with the solid’s mass and also with the physical properties of the gas such as its density and temperature. As shown in section 2, changes in the gas temperature and density will affect the mean thermal velocity and also the mean free path of the gas molecules. Such changes show their effects in the drag force of the gas through its Reynolds number and also through the relative velocity of the solid and result in different times of migration. An analytical study of the general dependence of the rate of migration on the physical properties of the solids and the nebular gas is currently under way.

As mentioned earlier, our motivation for initiating this study was to seek the possibility of the application of the results to the formation of planetesimals in marginally-gravitationally unstable disk models. As shown by Boss (2000), the disk instability scenario suggests rapid formation of giant gaseous protoplanets followed by sedimentation of small solids at the location of spiral arms and clumps of a gravitationally unstable disk all in about one thousand years. In our study, we considered a simple model of the solar nebula in order to focus our attention solely on the time of migration of solids and their variations with physical parameters of the system. Our results indicate that it is, indeed, possible for solids within certain ranges of size and density to migrate quite rapidly to the locations of maximum values of the gas density. For the model studied here, solids with densities of a few g cm^{-3} and with radii ranging from several centimeters to a few meters, migrate a radial distance of 1 AU during a time ($\sim 10^3$ years) comparable with the giant planet formation timescale implied by the disk instability model.

Regardless of whether disk instability can form gas giant planets, the likelihood that the solar nebula was marginally-gravitationally unstable implies that the processes studied here may have enhanced the growth rates of solid planetesimals.

At the end we would like to mention that the calculations in this study have been done for two dimensional motions and in a solar nebula that may not fully reflect the properties of a more realistic environment. In this study, we focused on the motion of solids as isolated objects without including their mutual interactions. To obtain a better understanding of the dynamics of solids and the times of their migrations, it is necessary to extend such an analysis to a three dimensional case and to allow for interactions between the objects. It is also important to consider temperature and density distributions for the nebular gas that portray the physical properties of a gravitationally unstable disk in a more realistic way. Such considerations are currently under way.

This work is partially supported by the NASA Origins of the Solar System Program under Grant NAG5-10547 and by the NASA Astrobiology Institute under Grant NCC2-1056.

REFERENCES

- Adachi, I., Hayashi, C., & Nakazawa, K. 1976, *Prog.Theor.Phys.*, 56, 1756
- Boss, A. P. 2000, *ApJ*, 536, L101
- Epstein, P. S. 1924, *Phys.Rev.*, 23, 710
- Inaba, S., & Wetherill, G. W. 2002, to appear in *Proceedings of Scientific Frontiers in Research on Extrasolar Planets (PASP)*
- Iwasaki, K., Tanaka, H., & Emori, H. 2001, *Pub.Astron.Soc.Japan*, 53, 321
- Kennard, E. H. 1938, *Kinetic Theory of Gases* (New York: McGraw-Hill)
- Kiang, T. 1962, *MNRAS*, 123, 359
- Landau, L. D., & Lifshitz, E. M. 1959, *Fluid Mechanics* (London: Pergamon Press)
- Malhotra, R. 1993, *Icarus*, 106, 264
- Pollack, J. B., Hubickyj, O., Bodenheimer, P., Lissauer, J. J., Podlak, M., & Greenzweig, Y. 1996, *Icarus*, 124, 62
- Probstein, R. F., & Fassio, F. 1969, *Am.Inst.Aeronaut.Astronaut.J*, 8, 4
- Supulver, K. D., & Lin, D. N. C. 2000, *Icarus*, 146, 525
- Weidenschilling, S. J. 1977, *MNRAS*, 180, 57
- Whipple, F. L. 1964, *Proc. Nat. Acad. Sci.*, 52, 565
- Whipple, F. L. 1972, in *From Plasma to Planets*, ed. A. Elvius (London: Wiley)

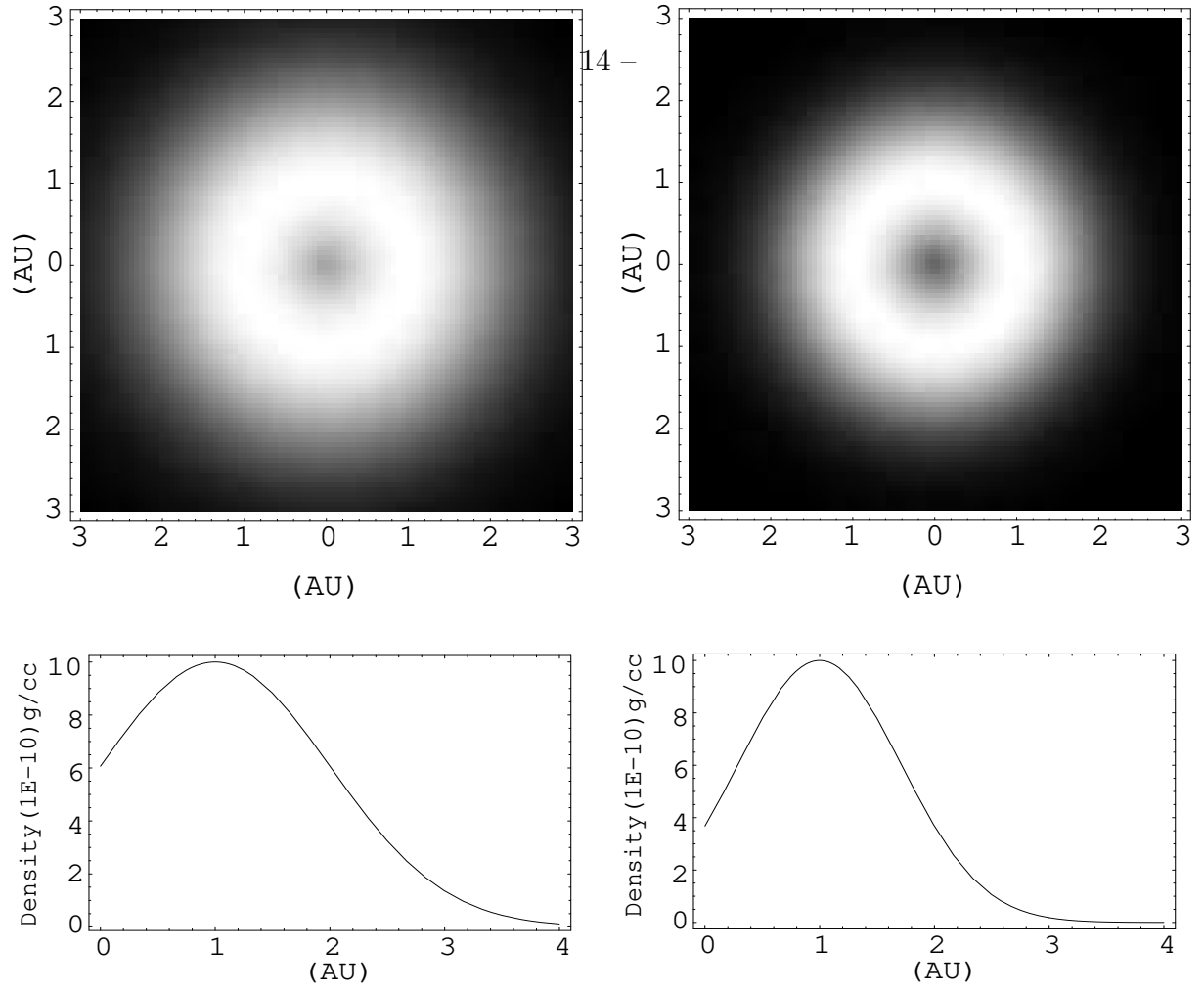


Fig. 1.— Graphs of the density of the gas for $\alpha = 0.5$ (left) and $\alpha = 1$ (right) in the disk midplane.

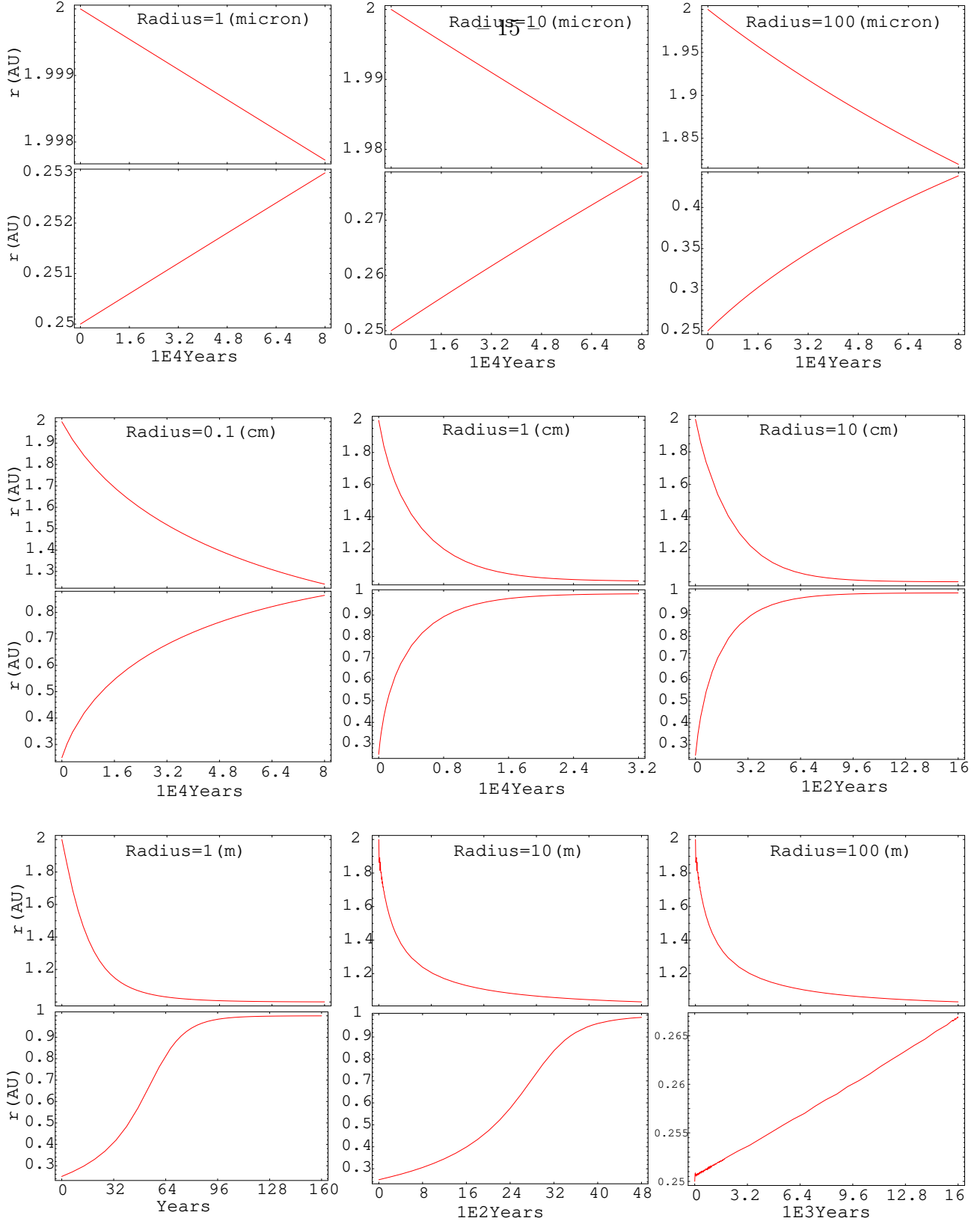


Fig. 2.— Migration of solids with radii ranging from 1 micron to 100 m and solid particle densities equal to 2 g cm^{-3} . The disk is isothermal at 1000 K and its density is given by equation (17) with $\alpha = 1$.

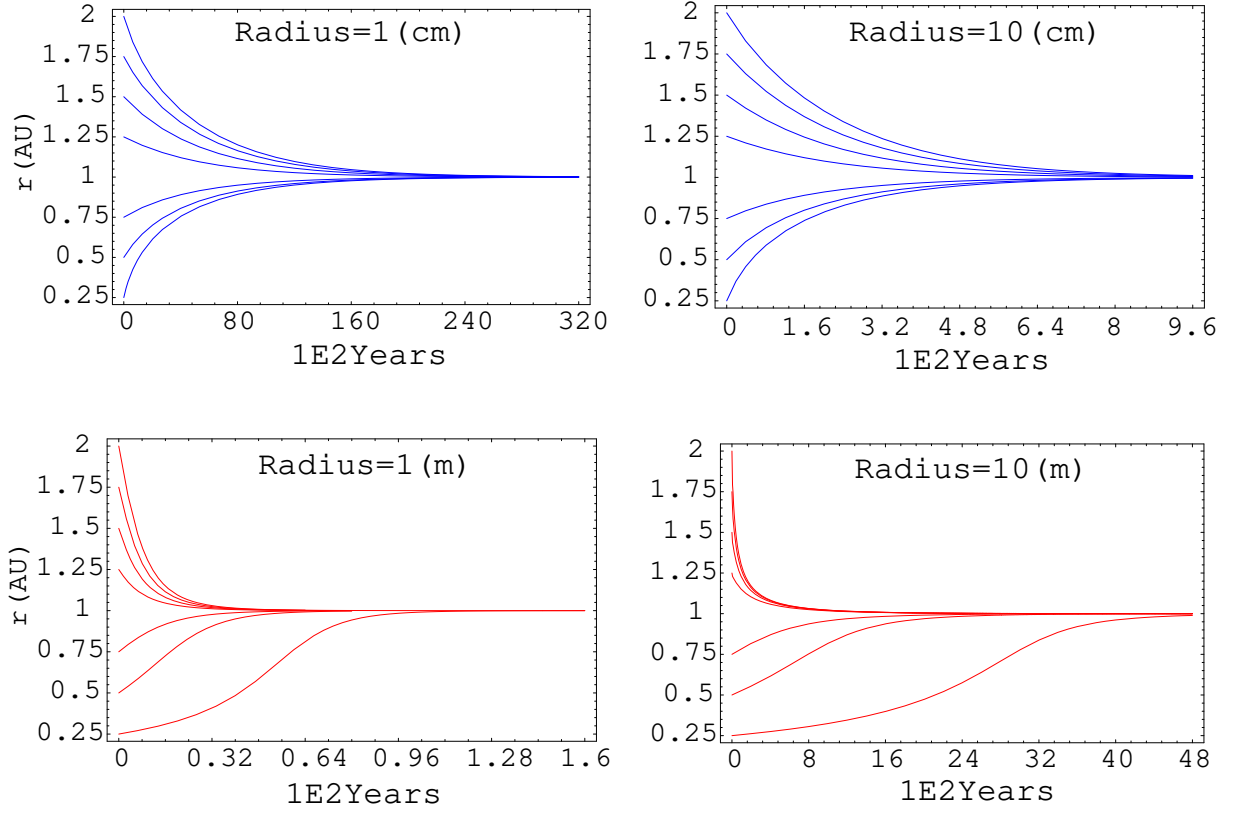


Fig. 3.— Among the solids of Figure 1, the ones with 10 cm to 10 m radii undergo rapid migrations.

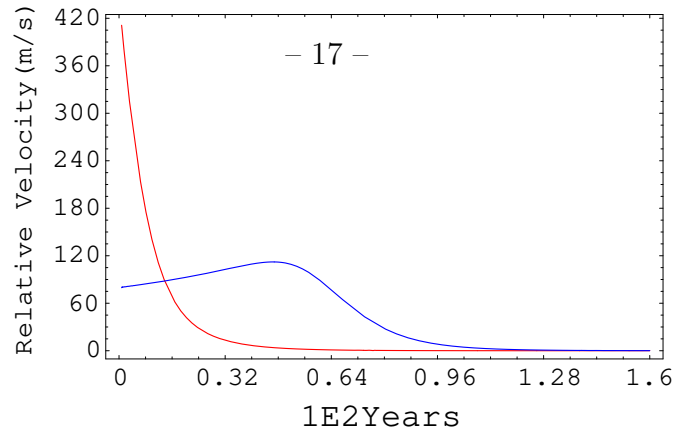


Fig. 4.— Relative velocity of a 1 m-sized solid while migrating inward from 1.75 AU (red) and outward from 0.25 AU (blue) to $r = 1$ AU.

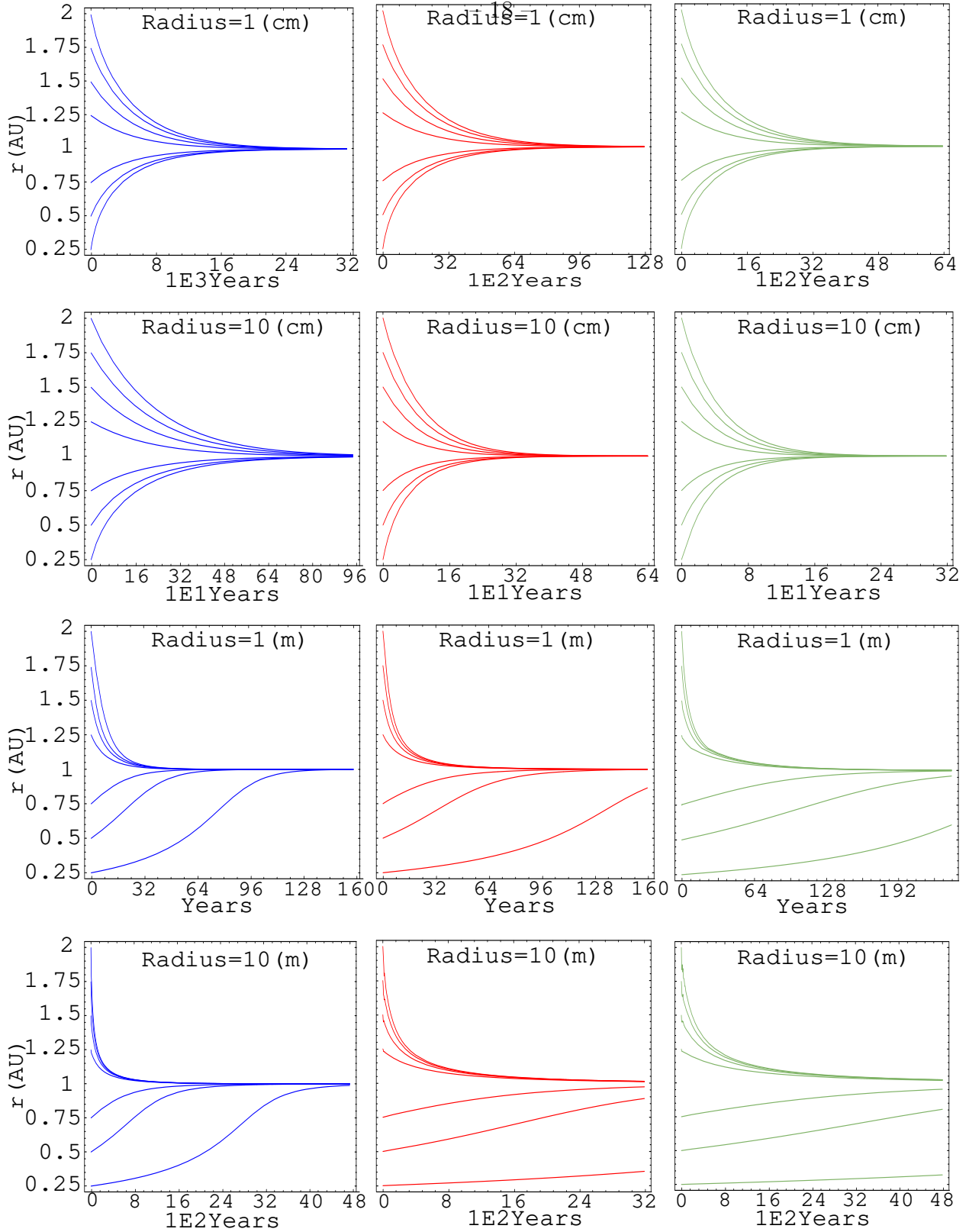


Fig. 5.— Migration of solids with densities equal to 2 g cm^{-3} (left column), 5 g cm^{-3} (middle column) and 10 g cm^{-3} (right column).

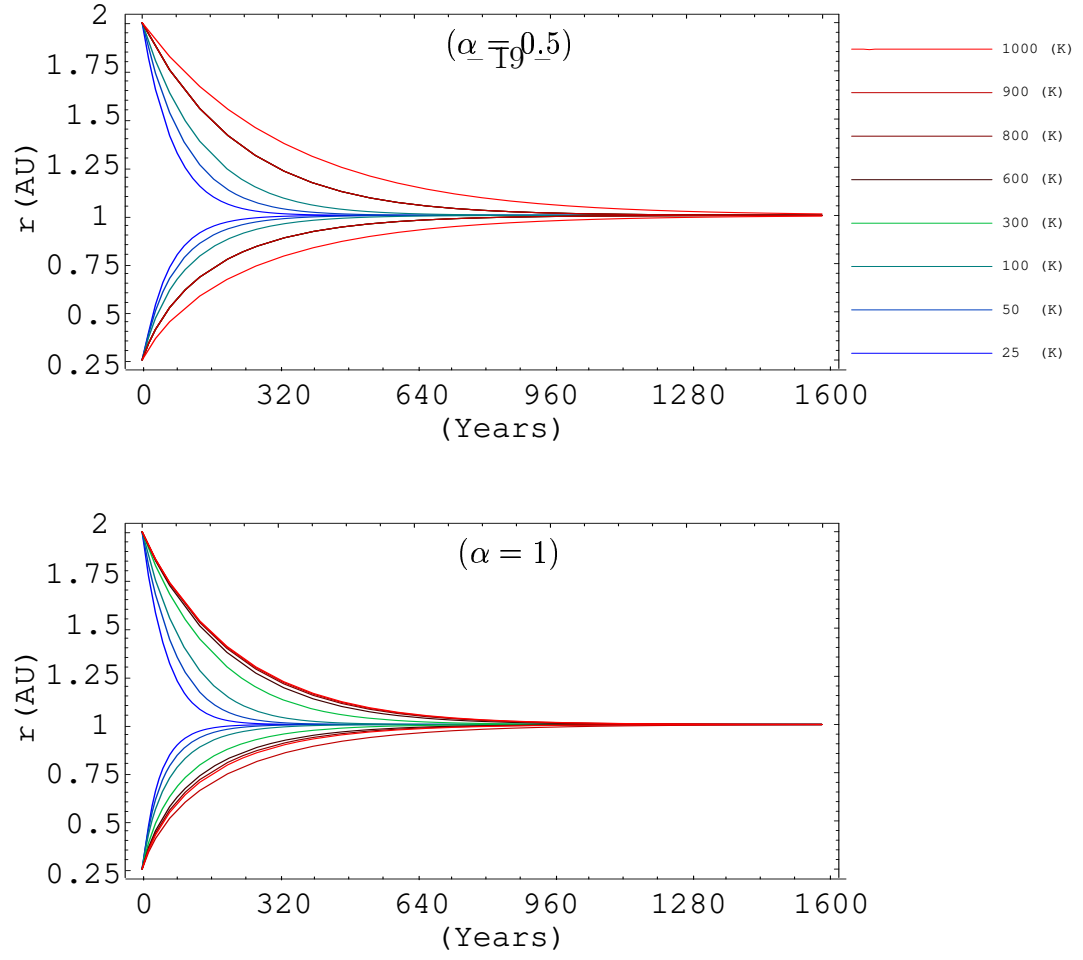


Fig. 6.— Migration of a solid at different temperatures. The radius of the object is 10 cm and its density is equal to 2 g cm^{-3} . As seen from this figure, the rate of migration decreases with increasing the temperature.

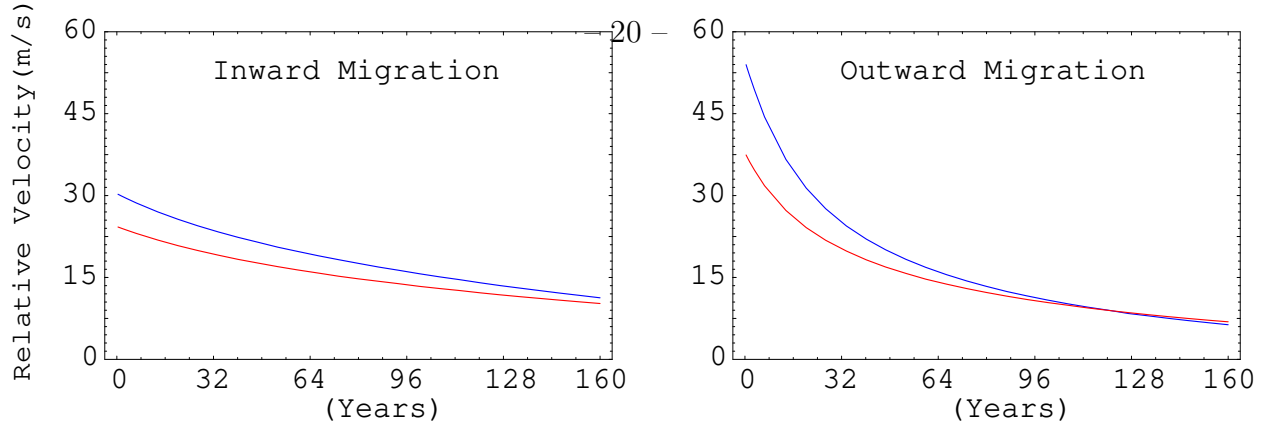


Fig. 7.— Relative velocity of a 10 cm-sized particle with a density of 2 g cm^{-3} migrating in a disk with a temperature equal to 300 K (blue) and 1000 K (red).